RSC Advances

Volume 1 | Number 1 | Jan 2013 | Pages 1–100

RSC Advances

www.rsc.org/advances

ROYAL SOCIETY OF CHEMISTRY

ROYAL SOCIETY OF CHEMISTRY

www.rsc.org/advances

Journal Name

ARTICLE

Bioactive calcium silicate extracts regulate the morphology and stemness of human embryonic stem cells at initial stage

Fan Zhang[a,b,c†], Dongyuan Lü[a,b,c†], Haiyan Li[d], Chunhua Luo[a,b,c], Jiang Chang[e‡], and Mian Long[a,b,c‡]

Embryonic stem cells (ESCs) are undifferentiated cells that have the capacity to self-renew and differentiate into a variety of cells and provide cell sources for regenerative medicine or biological specimens for cytotoxicity tests. Calcium silicate (CS), a bioactive silicate ceramic, can stimulate the osteogenic differentiation of various types of stem cells, but its role in regulating the biological phenotypes of ESCs remains unclear. Here, the impact of CS on human ESCs was investigated using CS-supplemented medium. The cytotoxicity of CS to hESCs and its effects on apoptosis, growth, proliferation, and differentiation were quantified systematically. Morphological analysis of hESC colonies indicated that the bioactive ions released from CS have little cytotoxicity to hESCs at two CS concentrations. Immunofluorescence and flow cytometry analyses showed that apoptosis was time-independent at early or late stages of hESC growth. In contrast, CS ion extracts regulated hESC differentiation in a time-dependent manner: ESC stemness was preserved by enhancing Oct-4, Sox-2, and Nanog gene expression at day 3, while the cells tended to differentiate at day 6. Combined tests on gene and protein levels further indicated that hESCs tended to differentiate into mesoderm in the presence of CS ion extracts, especially at low CS concentrations. These results demonstrate the effects of CS extracts on hESC stemness and differentiation at the molecular and cellular levels, suggesting that CS-based biomaterials could serve as a potential regulator for ESCs in regenerative medicine.

Introduction

Embryonic stem cells (ESCs) are pluripotent cells that can differentiate into most cell types of the three germ layers. ESCs have the potential to provide an unlimited source of cells for biomedical applications, including promoting tissue or organ regeneration for a broad spectrum of human diseases, elucidating mechanisms that underlie cell fate specification, and developing in vitro models for determining the metabolic and toxicological features of new drugs[1, 2]. Most potential applications require lineage-specific differentiation of ESCs into organ-specific cell types. To date, in vitro induction of ESC differentiation has been achieved through modulating the biochemical microenvironment of ESCs by adding specific growth factors[3], inducers[4], or repressors[5].

Biomaterials play a critical role in tissue regeneration. Some bioactive materials are able to stimulate differentiation of stem cells by releasing bioactive inorganic ions[6-8]. Si is an important element for mammals. For example, reduced amounts of collagen were found in silicon-deficient chicks and dietary silicon intake was good for bone mineral density in men and premenopausal women[9]. A serial of calcium-silicate based bioceramics, including bioglass, calcium silicate, dicalcium silicate, tricalcium silicate, akermanite, and others is known to affect the behaviors of stem cells in the past two decades. Once they contact with body fluid, all of these bioceramics can produce ionic products containing calcium ions, silicon ions, and some of them can even produce trace element ions such as magnesium ions, zinc ion, and others. Our studies and others demonstrated that the ionic products of these silicate bioceramics could stimulate proliferation and osteoblastic differentiation of various types of stem cells, including human bone marrow-derived stromal cells[10-14], adipose-derived stem cells[15, 16], human dental pulp cells[17], periodontal ligament cells[18, 19], human urine-derived stem cells[20], and human induced pluripotent stem cells[21]. Consequently, it is crucial to elucidate how these bioceramics regulate the biological features of human embryonic stem cells, a key cell type in basic sciences and biomedical application.

Specifically, calcium silicate (CS) is a new type of Ca-Si bioceramic biomaterial. CS bioceramics efficiently stimulate the viability[22, 23], adhesion[22-24], proliferation[22, 23, 25-27],

a. Center of Biomechanics and Bioengineering, Institute of Mechanics, Chinese Academy of Sciences, Beijing 100190, China
b. Key Laboratory of Microgravity (National Microgravity Laboratory), Institute of Mechanics, Chinese Academy of Sciences, Beijing 100190, China.
c. Beijing Key Laboratory of Engineered Construction and Mechanobiology, Institute of Mechanics, Chinese Academy of Sciences, Beijing 100190, China
d. School of Biomedical Engineering, Shanghai Jiao Tong University, 1954 Huashan Road, Shanghai 200030, China
e. Biomaterials and Tissue Engineering Research Center, Shanghai Institute of Ceramics, Chinese Academy of Sciences, Shanghai 200050, China
Electronic Supplementary Information (ESI) available.
See DOI: 10.1039/x0xx00000x
† Co-first authors: these authors contributed equally to this work.
‡ Corresponding authors.

ARTICLE

Journal Name

differentiation[22, 23, 25, 27, 28], and gene expression[28] of cells, and can be used to regenerate bone tissue or in biomedical applications related to osteogenesis, angiogenesis, and endodontics by release of Si/Ca-containing ionic products[7, 24]. CS induces osteogenic differentiation and angiogenesis in various cell types, such as mouse mesenchymal stem cells (mMSCs)[27], rat MSCs[29, 30], human MSCs[22, 31-35], mouse embryonic osteoblasts MC3T3-E1[36], osteoblasts[37-39], human adipose tissue-derived stem cell (ASCs)[26, 38, 40], human dental pulp cells (hDPCs)[33, 41], human orofacial mesenchymal stem cells (hOFMSC)[28], and human umbilical vein endothelial cells (HUVECs)[30, 35]. Thus, it is reasonably hypothesized that CS and its ionic extracts may have the potential to affect the growth and differentiation of embryonic-derived stem cells.

Considering the significance of ESC pluripotency, we designed the current study focusing on the effects of CS on ESC behaviors to elucidate how Si/Ca-biomaterials intrinsically manipulate cell differentiation fate. To our knowledge, the role of CS extracts in regulating the functions of ESCs has not been determined yet. In a basic science context, the most striking issue might be whether CS extracts are able to affect the stemness maintenance and directed differentiation of ESCs. To isolate the intrinsic impacts of CS, those biochemical stimuli or inducers used for directing ESC differentiation were excluded.

From a biomedical application viewpoint, the biocompatibility of Si/Ca-biomaterials is a prerequisite for developing pluripotent ESCs. CS bioceramics release Si and Ca ions into solution, and thus their cytotoxicity to ESCs and their contribution to apoptosis are critical. In this study, we analyzed the cytotoxicity, morphological changes, pluripotency and differentiation marker expression of human ESCs in the presence of CS extracts.

Experimental

CS extract preparation

CS powders were prepared by a chemical co-precipitation protocol previously described[42]. Briefly, continuous mixing of an aqueous solution of Na_2SiO_3 (1 mol l-1) with an aqueous solution of $Ca(NO_3)_2$ (1 mol l-1) at ambient temperature was carried out overnight (mol ratio: $Ca_2SiO_3:Ca(NO_3)_2$ = 1:1). After stopping the stirring, the resulting CS suspension was filtered and washed first with deionized water and subsequently with ethanol. After drying at 80°C overnight and baking at 800°C for 2 h, the CS powder was sieved to obtain particles between 100 and 150 μm for future use.

The extracts of CS bioceramics were prepared using a previous protocol[42]. Briefly, 1 g of bioceramic powder was soaked in 5 ml serum-free DMEM-F12 (GIBCO, USA) and incubated in a humidified 37°C/5% CO_2 incubator for 24 h. The supernatant was collected, sterilized through a filter (Millipore, 0.22 μm diameter), and stored at 4°C (ISO10993-1) for further use[6]. Here, the calcium silicate extract is referred to as CS extract. The CS extract was diluted with supplemented PSC (Pluripotent Stem Cell) easy iPS medium (PSCeasy), (CELLAPY,

China) at the ratios of 1/64 and 1/256, which was used for culturing the hESCs.

Ca, Si and P ion concentrations in CS extracts were then determined. Here 5 ml diluted samples taken from the culture media were analyzed by inductively coupled plasma atomic emission spectroscopy (ICP-AES; Optima 3000DV, Perkin Elmer, USA). PSCeasy iPS medium was used as control.

Cells and reagents

H9 hESCs were grown under serum-free conditions using PSCeasy iPS medium [modified essential 8 medium] (Cellapy, Beijing China). The composition of the medium is DMEM/F12, L-ascorbic acid, selenium, transferrin, $NaHCO_3$, insulin, FGF2, and NODAL. The cells were cultured in 6-well plastic plates (Tissue culture treated, Nunc, USA) that were pre-coated with 1.12% Matrigel diluted in DMEM/F12. After limited passages for expanding, the cells were frozen in liquid nitrogen or used directly in the functional experiments. The frozen cells were then thawed and maintained in a humidified, 95% air, 5% CO_2, 37°C incubator, with media changes every day. After cell passaging, the percentage of Oct4$^+$ cells was determined by flow cytometry (FACS), which is defined as the seed case. Oct4$^+$ cells were kept in the same PSCeasy iPS medium for one day, then transferred to CS-supplemented medium for an additional three or six days at two CS concentrations. Time points are denoted as (1+3) or (1+6) days, respectively. Alexa Fluor 488-conjugated rabbit-anti-human anti-Oct-4 monoclonal antibodies (mAbs), Fluor 594-conjugated rabbit-anti-human anti-Sox2 mAbs, and Fluor647-conjugated rabbit-anti-human anti-Nanog mAbs were purchased from Cell Signaling Technology (USA). TRITC-labeled phalloidin was purchased from RB-Sigma (USA) to stain the actin cytoskeleton. Hoechst 33342 from Enzo (USA) was used to stain cell nuclei[43].

Immunological staining and confocal microscopy

Expression levels of typical stemness biomarkers Oct-4, Sox2, and Nanog were visualized by confocal microscopy. hESCs cultured on plates were rinsed in PBS at pH 7.2, fixed for 15 min in 4% paraformaldehyde, and permeabilized with 0.4% Triton X-100 for 15 min. The cells were co-stained with Fluor-labeled anti-Oct-4, anti-Sox-2, and anti-Nanog mAbs, diluted at 1:40, 1:50, and 1:50, respectively, in 1% bovine serum albumin/PBS (to block nonspecific epitopes) at 4°C overnight. In some cases, TRITC-labeled phalloidin was used at a concentration of 5 μg/ml to stain actin. The samples were incubated with Hoechst 33342 for 10 min at room temperature (RT), washed 3-5 times with PBS, and stored at 4°C for examination with confocal laser scanning microscopy (Zeiss L710, Germany)[44].

Confocal microscopy was also used to measure apoptosis using a TUNEL kit. Briefly, hESCs cultured for (1+3) or (1+6) days were fixed using 4% paraformaldehyde. After being permeabilized by 0.1% TritonX100 followed by blocking with 1% BSA, the cells were incubated with 3'-OH terminal deoxynucleotidyl transferase to catalyze FITC-labeled dUTP binding to the OH groups of ruptured DNA from apoptotic

cells. Cell nuclei were stained with DAPI prior to confocal imaging and apoptotic cells were counted manually.

We also used the ImageJ software to calculate the relative fluorescence intensity (RFI) of various biomarkers. Here the contour and the projected area of those cells in a colony were defined from their actin-staining images. RFI was then measured within each cell area for the different biomarkers.

SEM imaging

hESCs were cultured in CS-supplemented PSCeasy iPS medium for (1+3) days, while cells grown in CS-free PSC medium served as controls. After being washed three times in Ca^{2+}- and Mg^{2+}-free PBS, the cells were fixed with 0.25% glutaraldehyde at RT overnight. After removing the glutaraldehyde with deionized water, fixed cells were dehydrated in an ethanol gradient and finally dried in a vacuum for 4 h. Image acquisition and analysis were performed using a scanning electron microscope (SEM) (FEI Quanta 200).

Flow cytometry

Expression of stemness markers was tested using flow cytometry. At the pre-set time points, cell colonies were dissociated with 0.25% trypsin. Collected cells were fixed for 10 min in 4% paraformaldehyde and permeabilized in 90% cold methanol. After being rinsed in PBS twice, the cells were incubated with labeled anti-Oct-4 (1:50 dilution) for 1 h at RT and then were analyzed using a FACS Canto II flow cytometer (Becton Dickinson, USA). To detect the percent of hESC apoptosis, we used the Annexin V-PE Apoptosis Detection Kit I (Becton Dickinson, USA) following the manufacturer's instructions and then performed flow cytometry analysis.

Real-time polymerase chain reaction (PCR) analysis

Real-time PCR was used to measure the gene expression of stemness biomarkers. Total RNA was extracted using the Trizol Reagent (Tiangen, China) from cells cultured in the PSCeasy or CS-supplemented PSCeasy iPS medium. RNA concentration was determined by measuring the optical absorbance (OA) of the extract at 260 nm, and RNA quality was determined by the OA ratio at 260 nm/280 nm. First strand complementary DNA (cDNA) was synthesized from 2 μg RNA using a First Strand cDNA Synthesis Kit (Toyobo, Japan). Real-time PCR was performed using a quantitative real-time amplification system (Mastercycler ® Rep, Realplex4, Eppendorf, Germany) following the manufacturer's protocol. A total volume of 20 μl amplification mixture per well was amplified as follows: 98°C for 10 s, 52°C, 60°C, 65°C annealing temperature for 10 s, and 72°C for 30 s. Biomarker genes for the pluripotency markers Oct-4 and Nanog, endoderm differentiation markers Bra and Foxa2, and mesoderm differentiation marker alkaline phosphatase (ALP) and Runx2, were evaluated. Actin was used as an internal control (Table S1). The comparative expression levels for each gene were normalized to actin[45].

Statistical analysis

Student's two-tailed t-test was performed to determine the statistical significance of differences between any two of the three groups for cell proliferation, morphology, stemness, and differentiation.

Results

Effect of CS extracts on the immobilization, growth and apoptosis of hESC colonies

To guarantee hESCs adhered well on the plate substrate, the cells were first placed in plain PSCeasy iPS medium for one day to keep the cells attached and grew up before being switched to CS-supplemented PSCeasy iPS medium at 1/256 or 1/64 CS extract dilution for an additional 3- or 6-day culture, that is, the cases of (1+3) or (1+6) days. Cytotoxicity of CS extracts to hESCs was evaluated by visualizing colony formation and daily growth. hESCs grew immobilized on the Matrigel, and the cells continued to grow well in PSC medium for up to 6 days (Fig. 1).
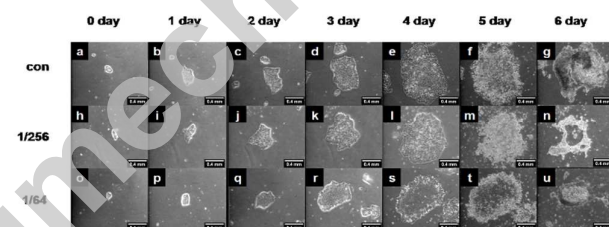

Fig. 1 Typical optical images for hESC H9 colonies on Matrigel. All colonies were first placed in plain PSCeasy iPS medium for one day, and then cultured in plain (1st row), 1/256 (2nd row), or 1/64 (3rd row) CS-supplemented PSCeasy iPS medium for additional six days. Scale bar = 400 μm.

Daily observation of the growth of hESCs colonies demonstrated that, at either 1/256 or 1/64 dilution of CS extract in short- (1+3 days) or long-period (1+6 days) culture, ESC colonies grew normally (2nd and 3rd rows) and showed a similar morphology to cells in plain PSCeasy iPS medium (1st row), suggesting that CS extracts do not produce extra cytotoxicity.

To further visualize the colony morphology and the membrane interconnection between adjacent hESCs, SEM analysis was performed, typically at day (1+3). Most of the individual hESCs inside the colony showed a typical globular configuration, and significant morphological changes were found in cells growing in the three different media (Fig. 2).
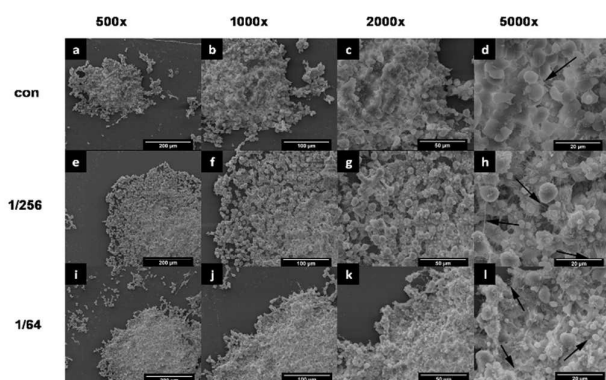
ARTICLE

Journal Name

Fig. 2 Typical SEM images for hESC H9 colonies on Matrigel. All colonies were first placed in plain PSCeasy iPS medium for one day, and then cultured in plain (1st row) or CS-supplemented (2nd and 3rd rows) PSCeasy iPS medium for additional three days. The magnification was indicated on the top of images. Typical 4-5 colonies were observed in each condition. Arrow heads denote the filament interconnections between adjacent hESCs.

More globular structures and many filamentous connections were observed between cells after CS treatment, indicating that hESCs become highly interconnected in the presence of CS extracts (3rd column).

Combined with those optical images for short-period (1+3 days) cultured cells (Fig. S1), these data indicated that hESCs grow well in the presence of CS extracts for ≥ 6 days before apoptosis (Figs. 1, 2, and S1). Thus, hESC colony immobilization and growth occur in CS-supplemented medium, with better interconnection among cells in the colony.

hESC colonies are not able to grow up infinitely but, instead, undergo apoptosis with time. Flow cytometry analysis indicated that, in a typical short-period culture (1+3 days), ≥ 87% cells were viable, and the percent apoptosis was comparable for all three conditions (Fig. S2a). Statistical analysis confirmed no differences when tests were repeated, regardless of slightly more severe than mild apoptosis in 1/64 CS-supplemented medium (Table 1).

Table 1   Summarized apoptosis percentages for hESC H9 cells.[†]

	Apoptosis percentage at 1+3 days			Apoptosis percentage at 1+6 days		
	Negative	Mild	Severe	Negative	Mild	Severe
Con	89.6±0.6%	4.4±0.6%	4.9±0.5%	38.4±6.0%	8.2±1.0%	46.6±6.1%
1/256	90.2±1.2%	4.3±1.6%	4.6±0.5%	32.0±17.3%	9.2±3.3%	54.8±16.6%
1/64	89.5±1.4%	4.0±0.8%	5.4±0.9%	42.4±9.4%	9.6±1.4%	44.0±8.8%

†: All colonies were first placed in plain PSCeasy iPS medium for one day, and then cultured in plain, 1/256, or 1/64 CS-supplemented PSCeasy iPS medium for additional three or six days. Cell apoptosis was determined using flow cytometry. Data were obtained from three repeated tests and each test has three repeats.

Here *negative* means little or null apoptosis, *mild* denotes low apoptosis, and *severe* defines high apoptosis. By contrast, the apoptosis percentage was higher in a typical long-period culture (1+6 days), where > 50% cells undergo apoptosis, mainly due to the lack of space for epitaxial growth and central necrosis mediated by an insufficient nutrient supply (Figs. 1 and S2b). While a high severe apoptosis percentage appeared in the 1/256 CS-supplemented medium (Fig. S2b and Table 1), this value varied in the repeated tests and no significant difference was found among the three cases (Table 1). Moreover, although the mild apoptosis percentage was slightly

higher in the 1/64 CS-supplemented medium than in control medium, this value was smaller and was not significant (Table 1). To further test the potential cytotoxicity of CS extracts on hESCs, additional immunostaining imaging was conducted using confocal microscopy for mild apoptosis. Again, no significant differences were found in either the quantity (Table S2) or the distribution (Fig. S3) of apoptotic cells inside the colonies. These combined data further supported that CS extracts are not cytotoxic to hESC H9 cells.

Impact of CS extracts on the morphology of hESC colonies

To test the potential morphological change of hESCs in the presence of CS extracts, the morphological parameters of colony circularity (= $4\pi[\text{area}]/[\text{perimeter}]^2$) and aspect ratio (= major axis/minor axis) were estimated from the daily optical images in long-period culture (1+6 days) and compared among the three growth conditions. No data on the final day were collected because most of the colonies detached. Colony circularity at the nth day (=2, 3,,, 6), normalized to the measurement on the 1st day, yielded a time course that fluctuated with time in each case (Fig. 3a-e).
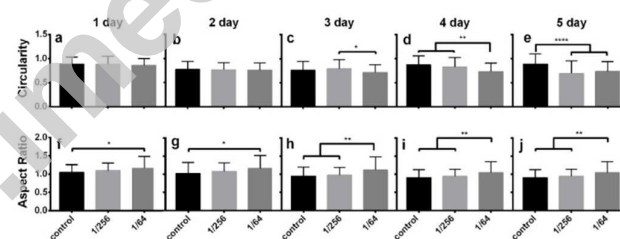

Fig. 3 Morphological analysis of hESC H9 colonies in plain (black bars), 1/256 (light grey bars), or 1/64 (dark grey bars) CS-supplemented PSCeasy iPS medium for long-period culture up to one plus six (1+6) days. Data are obtained from daily optical imaging in three repeated tests and presented as the mean ± standard deviation (SD) of circularity (a-e) and aspect ratio (f-j), respectively, for totally 60 colonies. Data for the cells in the presence of CS extracts were normalized to those in the absence of CS extracts for only one-day culture. Statistically significant difference, P < 0.05*, 0.01**, 0.001***, and 0.0001****.

While no difference was found among the three media conditions at the early stage (2nd-3rd days), the colonies became less round with lower circularity on the 4th day in 1/64 CS-supplemented medium, followed by a significant reduction on the 6th day in both 1/256 and 1/64 CS-supplemented media. By contrast, the colony aspect ratio on the nth day, normalized to the 1st day, decreased gradually with time in all cases, but no significant difference was found (Fig. 3f-j). A higher aspect ratio for colonies in the 1/64 CS-supplemented medium was first observed on the 1st-2nd days compared to cells grown in plain medium. The difference was further enlarged on the 4th-6th days compared to both plain and 1/256 CS-supplemented media. These results implied that the round shape of hESC colonies tended to transition to asymmetric growth and become long and narrow, especially after extended culture times and in high CS concentrations.

To further test morphological changes in hESC colonies, an immunostaining-based analysis was conducted using confocal

RSC Advances Accepted Manuscript

microscopy in short-period cultures (1+3 days). hESC colonies become long and narrow at later time points in all media conditions because the absolute circularity was reduced from unity to 0.48-0.51 and 0.39-0.50 at (1+3)th and (1+6)th days, respectively, while the absolute aspect ratio was enhanced from unity to 1.48-1.51 and 1.85-1.87 at (1+3)th and (1+6)th days, respectively (Fig. S4). Thus, CS-supplemented medium promotes asymmetric growth and long and narrow colony shapes over time.

Differentiation and stemness of hESCs in CS extracts

We further tested the impact of CS extracts on the capacity of hESCs to differentiate or maintain their stemness. We tested the concentration and time dependence of CS extracts on stemness biomarker expression at the gene and protein level. First, using Oct-4 as a marker to detect the percent of hESCs that maintained stemness after (1+3) day culture (Fig. 4a),
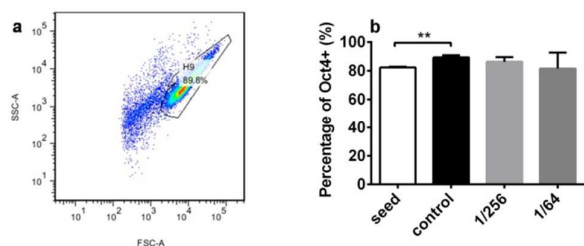

Fig. 4 Stemness maintenance of hESC H9 cells in plain (black bars), 1/256 (light grey bars), or 1/64 (dark grey bars) CS-supplemented PSCeasy iPS medium for short-period culture at one plus three (1+3) days. A typical flow cytometry analysis is illustrated for target cells stained by anti-Oct-4 mAbs and gated in the scatter plot (black line) (A). The percentage of Oct-4$^+$ H9 cells is also compared using histograms under different conditions (B) where seed case (white bars) denotes the Oct-4$^+$ percentage of passaged cells prior to seeding on Matrigel. Data are presented as the mean ± SD in triplets under each condition.

we observed that approximately 90% of cells were viable, and > 80% of them were positive for Oct-4 (81.3±10.7–89.0±1.5%) (Fig. 4b). Flow cytometry analysis indicated that either plain or CS-supplemented medium was able to maintain cell stemness. The percentage of Oct4$^+$ cells in the control case (day 1) was slightly higher than the seed case, which is consistent with colony growth in our daily observations (cf. Fig. 1).

Pluripotency, endoderm, and mesoderm genes were tested using qPCR to explore the potential directed differentiation of hESCs in the presence of CS extracts. In the short-period culture ((1+3) days), the expression of the Oct-4 and Nanog genes was similar in the absence or presence of CS extracts (Fig. 5a, b),
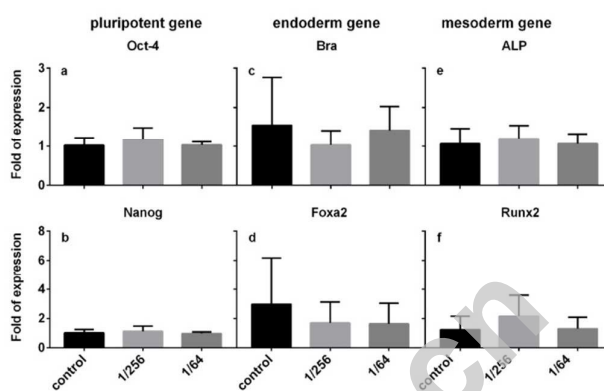

Fig. 5 Gene expressions of hESC H9 cells in plain (black bars), 1/256 (light grey bars), or 1/64 (dark grey bars) CS-supplemented PSCeasy iPS medium for short-period culture at one plus three (1+3) days. Cell differentiation is determined using qPCR assay for pluripotency genes Oct-4 and Nanog (1st column), endoderm genes Bra and Foxa2 (2nd column), and mesoderm genes ALP and Runx2 (3rd column). Data are presented as the mean ± SD of fold of expression in two independent measurements in six replicates under each condition.

consistent with the flow cytometry analysis of Oct-4$^+$ cells (cf. Fig. 4). Our data support that hESCs maintain their stemness well in short-period culture. Additionally, the expression of the endoderm Bra and Foxa2 genes was lower in 1/256 or 1/64 CS-supplemented medium than in plain medium, even though no significant differences were found (Fig. 5c, d). These data suggest that CS extracts are not favorable for endodermal differentiation. By contrast, the expression of mesoderm markers ALP and Runx2 was higher in 1/256 CS-supplemented medium than in 1/64 CS-supplemented or plain medium (especially for the osteogenic marker gene Runx2) (Fig. 5e, f). These data imply that CS extracts might initiate hESC mesodermal differentiation. Our results indicate that hESCs maintain their stemness in short-period culture, but have the potential to be differentiated into mesodermal cells in the presence of concentrated CS extracts.

Finally, further direct comparisons were required to elucidate the impact of CS extracts on hESC stemness in both short- and long-period culture at the protein level. Using the three typical pluripotency markers Oct-4, Sox2, and Nanog to define the fate of hESC stemness or differentiation, immunostaining images were obtained in (1+3)- or (1+6)-day cultures grown in 1/256 or 1/64 CS-supplemented medium. All three markers were highly expressed in typical hESC colonies (Fig. 6).
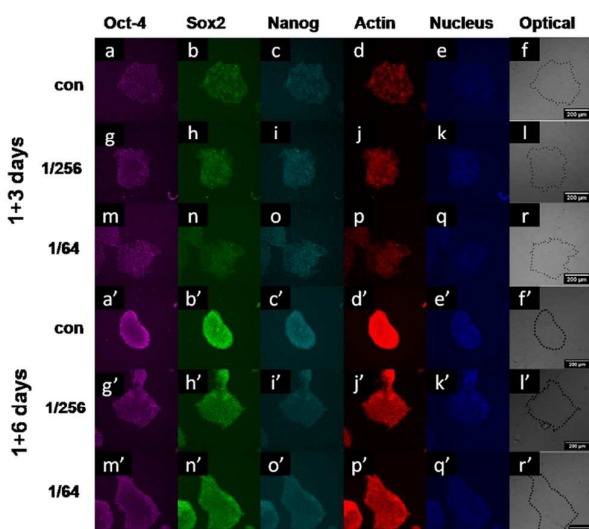
Fig. 6 Typical immunostaining images of hESC H9 cells in plain, 1/256, or 1/64 CS-supplemented PSCeasy iPS medium for short- ((1+3) days; 1st-3rd rows) or long-period ((1+6) days; 4th-6th rows) culture. Multiple pluripotency biomarkers of Oct-4 (1st column), Sox2 (2nd column), and Nanog (3rd column) were visualized by confocal microscopy under three conditions when actin (4th column) and nucleus (5th column) staining as well as optical images (6th column) serve as reference. Black dotted lines illustrate the contour of the colonies. Scale bar = 200 μm.

The mean relative fluorescence intensity (RFI) of each marker protein was estimated from the images and compared in the three growth conditions using actin as a reference. In short-period cultures, the RFI values were similar for Oct-4 (Fig. 7a)
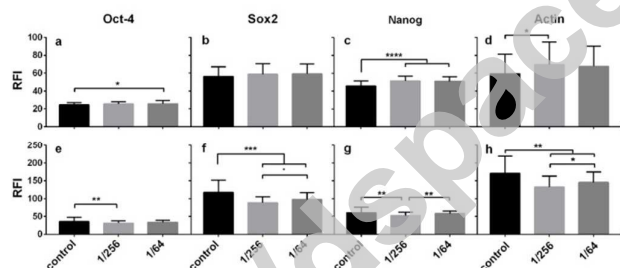

Fig. 7 Quantitative comparison of relative fluorescence intensity (RFI) for hESC H9 colonies in plain (black bars), 1/256 (light grey bars), or 1/64 (dark grey bars) CS-supplemented PSCeasy iPS medium for short- ((1+3) days; 1st row) or long-period ((1+6) days; 2nd row) culture. Data were calculated from three replicates and presented as the mean ± SD for totally ~60 colonies under each condition.

and Sox2 (Fig. 7b) and higher for Nanog (Fig. 7c) in the presence of CS extracts compared to controls. Again, we showed that hESC colonies are able to maintain their stemness after short-period culture in CS-supplemented medium. However, in long-period culture, CS treatment enhanced the RFI values for all of the three marker proteins (Fig. 7). The lowest RFI value was observed in the 1/256 CS dilution for Oct-4 (Fig. 7e), Sox2 (Fig. 7f), or Nanog (Fig. 7 g), and higher values were observed in the 1/64 CS dilution and control cells. Meanwhile, actin expression followed the same pattern, being higher in short-period cultures and lower in long-period cultures in the presence of CS extracts compared to controls. Taken together, these gene and protein data for short- and

long-period tests (Figs. 4-7) demonstrate that CS extracts maintain hESC stemness in short-period cultures, but in long-period cultures initiate hESC differentiation. The effects of CS were not dependent on the two concentrations used here, but on the culture period.

Proliferation of hESCs in CS extracts

For future biomedical applications, hESC proliferation dynamics under CS treatment should be quantified, not only for scaling-up production of source cells but also for the optimizing the time point at which the cells are collected. Here, daily proliferation was estimated by the colony projected area at the nth day subtracted from the first (n-1)th day and then divided by the (n-1)th day (n = 2, 3,,,6). Proliferation decreased with time in all three treatment conditions, suggesting that the proliferation capacity of hESC colonies was reduced. In fact, the majority of the colonies was detached on the final day (7th day). Comparing the proliferation difference at a given time point among three cases, we found that the proliferation rate exhibited a declining pattern with time. Specifically, the proliferation was lower on days 2, 5, and 6 in 1/256 CS-supplemented medium compared to plain or 1/64 CS-supplemented medium (Fig. 8).
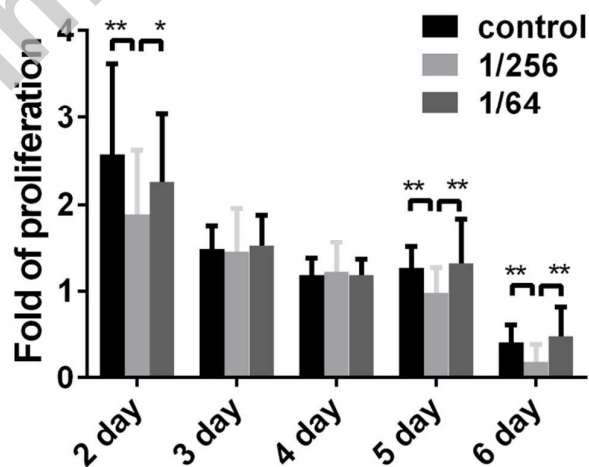

Fig. 8 Time course of hESC H9 colony proliferation in plain (black bars), 1/256 (light grey bars), or 1/64 (dark grey bars) CS-supplemented PSCeasy iPS medium long-period ((1+6) days) culture. Daily incremental fold of proliferation was estimated by the colony projected area at nth day subtracted by the one at (n-1)th day and then divided by the one at (n-1)th day (n = 2, 3,,,6). Data are presented as the mean ± SD of for totally 60 colonies under each condition, and the comparison under different conditions at given time points are also presented.

Combined with the data for hESC differentiation (cf. Fig. 5-6), our results suggest that high concentrations of CS extracts are beneficial for hESC proliferation, while low CS concentrations are favorable for differentiation.

Ion concentration of extracts

To elucidate the effects of ionic products on hESCs, the concentrations of the ions released from the CS ceramics to

Journal Name

ARTICLE

the extracts and diluted at different ratios with control medium were detected by ICP-AES. The results were summarized in Table 2.

Table 2   Ion concentration of CS extracts diluted at two ratios

	Ca (µg/ml)	P (µg/ml)	Si (µg/ml)
PSCeasy iPS medium	36.12	33.41	0.14
CS 1/256	36.40	33.64	0.47
CS 1/64	35.82	33.40	1.44

It can be seen that the Ca and P ion concentrations in CS extracts diluted at 1/64 and 1/256 were similar to those in control medium. However, the concentrations of Si ions in CS extracts diluted at 1/64 and 1/256 with PSCeasy iPS medium were 1.44 and 0.47 µg/ml, which were much higher than those in control medium (0.14 µg/ml). These results implied that functional differences of hESCs presented in CS extracts were mainly attributed to the changes of Si ions in distinct dilution.

Discussion

Although we have determined the effective ion concentrations of CS extracts on hESCs (Table 2), it still needs to keep in mind that the optimal *in vitro* concentration may not be the physiological concentration *in vivo*. As far as we know, the naturally occurring exposure concentration of silicon ions keep changed dynamically in different tissues or organs. A body of evidences indicates that serum Si concentration is ~0.1-0.2 µg/ml for most healthy adults[9, 46-49], is peaked at ~0.8-1.2 µg/ml after intake of silicon-containing food[9, 46, 47] and even yields 15-fold higher for hemodialysis patients up to ~3.3 µg/ml (their basal level is 0.9 µg/ml) when they take in silicon food[50]. In the current work, the plain medium used has similar silicon concentration in human physiological serum. 1/256 diluted medium presents a ~2-fold higher value, which can be treated as the effective concentration. 1/64 diluted medium yields a ~7-fold higher value, which is similar to the peak concentration for intake of silicon food from healthy adults and slightly higher than the low end from hemodialysis patients. Collectively, the rationale of our design in Si concentration is to present the sufficient effects of CS extracts and reduce the potential damage on hESCs, as possible, in a relatively long duration.

Long term goal of our work is to screen specificity of CS extracts in the regulation of hESC fate and stimulate osteogenesis from ESCs. As the first step, we focus on the regulating mechanisms of CS extracts on self-renewal and differentiation at initial stage. We report the influence of calcium silicate bioceramics on the biological functions of hESCs. Little cytotoxicity and no additional apoptosis were observed in hESCs grown with CS extracts in the culture medium. The cells formed long and narrow colonies with defined shapes and proliferated at high CS concentrations for up to six days. hESCs maintained stemness in 1+3 days cultures, but low CS concentrations promoted differentiation into mesodermal cells in 1+6 days cultures. To the best of our

knowledge, this is the first work to systematically map the role of CS extracts in regulating the cytotoxicity, apoptosis, growth, proliferation, stemness and differentiation of hESCs using an in vitro approach.

The biological responses of embryonic stem cells to CS extracts are undoubtedly meaningful for both basic science and biomedical applications. When a novel biomaterial is applied to cultured cells, cytotoxicity is the first issue to be addressed. As we know, some Si-containing bioceramics have different cytotoxicity to cells. For example, crystal structures of $CaSiO_3$ polymorphs have high dissolution rate and induce high Si^{2+} concentration, which cause significant cytotoxicity to hMSC[51]. A new discoloration-resistant calcium aluminosilicate cement initially dissolve and produce $Ca(OH)_2$ and then induce high pH, which damage hDPSC seriously[52]. Thus, it is necessary to evaluate the cytotoxicity of CS extracts on human ESCs. We used two methods to detect whether CS ions in the medium have cytotoxicity to hESCs, where flow cytometry analyses usually denote the percentage of total living cells while TUNEL tests define the apoptosis of single cells. Both results show cooperatively that CS extracts do not induce apoptosis in hESC colonies (Tables 1 and S2; Figs. S2-S3). Thus, hESCs are able to grow in the presence of CS extracts and form well-defined colonies with normal shapes and better interconnectiveness. Importantly, the colonies' morphologies experience continuous changes from small, round shapes to longer, more asymmetric shapes in both 1+3 days and 1+6days cultures. It is evident that stem cell morphology is related to the feature of forming colonies. For example, multipotent trophoblast stem cells are able to form circular colonies but are shaped with polarized morphology in smaller circularity in the absence of FGF4 to undergo epithelial-mesenchymal transition[53]. In the current work, ESC colony morphology was found to be correlated with colony size. At early stages, most colonies are small, fully spread, and highly symmetrical. At later stages, colonies become irregularly shaped, mainly due to the limited space for growth[54]. Our data supports previous observations that ESC colonies with initially small, rounded shapes grew asymmetrically (Figs. 1 and S1). The presence of CS extracts induced longer and narrower colonies at high CS concentrations in 1+6 days cultures (Figs. 3 and S4). This well-defined colony formation and morphology could promote the normal proliferation of hESC colonies in the CS-supplemented medium, where daily proliferation was comparable in plain medium and high CS concentrations (Fig. 8). More interestingly, the connective filaments between individual hESCs were significantly enhanced in a concentration-dependent pattern when CS extracts were present (Fig. 2), presumably because CS extracts could up-regulate the expression of cadherin at the cell junctions[42]. This is especially meaningful for ESCs because ESC-specific growth requires strong interactions and close connections between neighboring cells.

The most striking impact of CS extracts on hESC colonies was in regulating their stemness maintenance and directed differentiation. While the literature contains no evidence on the impact of CS extracts on hESC omnipotency, a body of

evidence demonstrates how biochemical or biomechanical factors modulate the fate of stem cells. On one hand, CS bioceramics and their analogs are able to direct the differentiation of hMSCs into osteoblastic cells[22, 23, 25, 27]. On the other hand, substrate stiffness, microtopography, and geometry are able to synergistically regulate the differentiation of ESCs[43] or even MSCs[44]. In this work, our data suggest that the 1+3 days culture of hESC colonies in the presence of CS extracts maintains cell stemness (Figs. 4-5), as cell-cell contact inhibits cell differentiation. After 1+6 days culture, however, tight connections between the cells prevents sufficient nutrient exchange inside the colonies, and stemness maintenance is compromised, and directed differentiation becomes initiative. This finding makes sense regarding the requirement that hESCs be kept at the undifferentiated stage before being used for biomedical applications. Additionally, the daily proliferation of hESC colonies was lower at low CS concentration than in plain or highly concentrated CS medium (Fig. 8), which seems to be in accordance with the capacity of CS to maintain stemness at low concentrations. 1+6 days culture tends to induce ESC differentiation into mesodermal cells (Figs. 6-7). This observation may be potentially helpful for bone regeneration and repair because bone cells are mesoderm-derived and the mesoderm can form bone and blood vessels during embryonic development. It should be pointed out that hESC subculture was not undertaken for several passage in the current work, even though hESCs are typically sub-cultured per 7 days. Here we just focused on the initial stage of CS extract's impact on hESC self-renewal and mesodermal differentiation mainly because these initial responses of hESCs in the presence of CS extracts is the pre-requisite for future passaged subculture.

Biocompatible and bioactive CS bioceramics can initiate the lineage-specific differentiation of stem cells via dissolving calcium and silicate ions in the culture medium[29]. For example, three ceramic materials in the Ca_2SiO_4-$Ca_3(PO_4)_2$ system could serve as potential osteogenic substrates onto which human mesenchymal stem cells can adhere, proliferate, and differentiate into osteoblasts[55]. One of the authors' labs has demonstrated that silicate-based biomaterials stimulate osteogenesis and angiogenesis. The Si/Ca ions released from the materials stimulate osteogenic differentiation of bone marrow mesenchymal[7, 56] or urine-derived stem cells (USCs)[57] and angiogenic differentiation of endothelial cells (ECs) when SC or EC are separately cultured[7, 57] or in a SC-EC co-culture[56] system. Here we report that hESCs tend to differentiate into mesodermal cells in the presence of CS extracts (Fig. 5), which is consistent with previous findings and could provide a new cell source for bone regeneration and repair.

While CS ions were found in the current work to regulate hESC differentiation, the underlying molecular mechanisms are still unclear and need to be further elucidated. In fact, many other types of stem cells are affected by CS ions through known signaling pathways. For example, pFAK-MAPK-ERK/Akt signaling plays an important role in inducing CS-treated stem cells to express differentiation biomarkers such as ALP and Runx2[7, 26, 30, 33, 35, 41, 57, 58]. The cells recognize the bioceramic materials and stimulate the phosphorylation of FAK, which in turn activates other protein kinases and accomplishes the biological effects[33]. It is still difficult, however, to isolate the specific effects of the extracted ions on this pathway from the direct influences of the CS biomaterials themselves. Additionally, our previous work also demonstrated that the Wnt/β-catenin pathway is a possible candidate responsible for the cellular response to CS ion stimulation[56] because Wnt/β-catenin signaling is critical in inducing osteogenic differentiation in USCs and in balancing the growth and differentiation of stem cells in the presence of CS ions[59, 60]. Similarly, by excluding the effects of Na ion, a specific Si concentration can stimulate osteogenic differentiation of BMSC and a few classic genes in Wnt/SHH pathways are upregulated, which is consistent with our previous results[61]. Such clues provide potential candidate signaling molecules for elucidating the effects of CS ions on ESC differentiation in future studies.

Conclusions

Calcium silicate induced a fate decision in hESCs exposed to CS extracts in vitro. The capacity to form cell colonies was altered in a time- and concentration-dependent manner. The underlying mechanism involves alterations to cell morphology, proliferation, stemness, and differentiation. Interestingly, CS extracts modulated stemness in short-period cultures but initiated directed differentiation in long-period cultures. These results imply CS materials extracts may be useful to enhance bone regeneration and repair, particularly if hESCs are considered a therapeutic cell source for regenerative applications.

Acknowledgements

Notes and references

1. J. A. Thomson, J. Itskovitz-Eldor, S. S. Shapiro, M. A. Waknitz, J. J. Swiergiel, V. S. Marshall and J. M. Jones, *Science*, 1998, **282**, 1145-1147.
2. B. E. Reubinoff, M. F. Pera, C. Y. Fong, A. Trounson and A. Bongso, *Nature biotechnology*, 2000, **18**, 399-404.
3. A. Kasahara, S. Cipolat, Y. Chen, G. W. Dorn, 2nd and L. Scorrano, *Science*, 2013, **342**, 734-737.
4. M. Borowiak, R. Maehr, S. Chen, A. E. Chen, W. Tang, J. L. Fox, S. L. Schreiber and D. A. Melton, *Cell stem cell*, 2009, **4**, 348-358.

Journal Name　　　　　　　　　　　　　　　　　　　　　　　　　　　　　　　　**ARTICLE**

5. E. Walker, W. Y. Chang, J. Hunkapiller, G. Cagney, K. Garcha, J. Torchia, N. J. Krogan, J. F. Reiter and W. L. Stanford, *Cell Stem Cell*, 2010, **6**, 153-166.
6. H. Li and J. Chang, *Acta biomaterialia*, 2013, **9**, 5379-5389.
7. K. Lin, L. Xia, H. Li, X. Jiang, H. Pan, Y. Xu, W. W. Lu, Z. Zhang and J. Chang, *Biomaterials*, 2013, **34**, 10028-10042.
8. A. Hoppe, N. S. Guldal and A. R. Boccaccini, *Biomaterials*, 2011, **32**, 2757-2774.
9. S. Heinemann, T. Coradin and M. F. Desimone, *Biomater Sci-Uk*, 2013, **1**, 688-702.
10. H. L. Sun, C. T. Wu, K. R. Dai, J. Chang and T. T. Tang, *Biomaterials*, 2006, **27**, 5651-5657.
11. Y. Huang, X. Jin, X. Zhang, H. Sun, J. Tu, T. Tang, J. Chang and K. Dai, *Biomaterials*, 2009, **30**, 5041-5048.
12. H. Lu, N. Kawazoe, T. Tateishi, G. Chen, X. Jin and J. Chang, *Journal of Biomaterials Applications*, 2010, **25**, 39-56.
13. M. L. Zhang, C. T. Wu, K. L. Lin, W. Fan, L. Chen, Y. Xiao and J. Chang, *J Biomed Mater Res A*, 2012, **100A**, 2979-2990.
14. Z. Chen, C. Wu, W. Gu, T. Klein, R. Crawford and Y. Xiao, *Biomaterials*, 2014, **35**, 1507-1518.
15. Q. H. Liu, L. Cen, S. Yin, L. Chen, G. P. Liu, J. Chang and L. Cui, *Biomaterials*, 2008, **29**, 4792-4799.
16. X. G. Liu, K. L. Lin and J. A. Chang, *Crystengcomm*, 2011, **13**, 1959-1965.
17. W. Peng, W. Liu, W. Zhai, L. Jiang, L. Li, J. Chang and Y. Zhu, *Journal of Endodontics*, 2011, **37**, 1240-1246.
18. Y. H. Zhou, C. T. Wu and Y. Xiao, *Acta biomaterialia*, 2012, **8**, 2307-2316.
19. C. T. Wu, Y. H. Zhou, C. C. Lin, J. Chang and Y. Xiao, *Acta biomaterialia*, 2012, **8**, 3805-3815.
20. J. Guan, J. Zhang, S. Guo, H. Zhu, Z. Zhu, H. Li, Y. Wang, C. Zhang and J. Chang, *Biomaterials*, 2015, **55**, 1-11.
21. X. X. Dong, H. Y. Li, Y. L. Zhou, L. Ou, J. K. Cao and J. Chang, *J Mater Chem B*, 2016, **4**, 2369-2376.
22. N. Zhang, J. A. Molenda, J. H. Fournelle, W. L. Murphy and N. Sahai, *Biomaterials*, 2010, **31**, 7653-7665.
23. P. N. De Aza, D. Garcia-Bernal, F. Cragnolini, P. Velasquez and L. Meseguer-Olmo, *Materials science & engineering. C, Materials for biological applications*, 2013, **33**, 4009-4020.
24. C. W. Wang, T. Y. Chiang, H. C. Chang and S. J. Ding, *Journal of materials science. Materials in medicine*, 2014, **25**, 2193-2203.
25. H. W. Li and J. Y. Sun, *J Int Med Res*, 2011, **39**, 112-128.
26. K. J. Kim, Y. A. Joe, M. K. Kim, S. J. Lee, Y. H. Ryu, D. W. Cho and J. W. Rhie, *International journal of nanomedicine*, 2015, **10**, 2261-2272.
27. S. Saravanan, S. Vimalraj, M. Vairamani and N. Selvamurugan, *Journal of biomedical nanotechnology*, 2015, **11**, 1124-1138.
28. M. G. Gandolfi, S. N. Shah, R. Feng, C. Prati and S. O. Akintoye, *Journal of endodontics*, 2011, **37**, 1102-1108.
29. A. El-Ghannam and C. Q. Ning, *Journal of biomedical materials research. Part A*, 2006, **76**, 386-397.
30. C. Wang, K. Lin, J. Chang and J. Sun, *Biomaterials*, 2013, **34**, 64-77.
31. L. Bjerre, C. E. Bunger, M. Kassem and T. Mygind, *Biomaterials*, 2008, **29**, 2616-2627.
32. S. J. Ding, M. Y. Shie, T. Hoshiba, N. Kawazoe, G. Chen and H. C. Chang, *Tissue engineering. Part A*, 2010, **16**, 2343-2354.
33. M. Y. Shie and S. J. Ding, *Biomaterials*, 2013, **34**, 6589-6606.
34. A. A. Eid, K. A. Hussein, L. N. Niu, G. H. Li, I. Watanabe, M. Al-Shabrawey, D. H. Pashley and F. R. Tay, *Acta biomaterialia*, 2014, **10**, 3327-3334.
35. C. Wang, K. Lin, J. Chang and J. Sun, *Journal of biomedical materials research. Part A*, 2014, **102**, 2096-2104.
36. S. Dong, J. Sun, Y. Li, J. Li, W. Cui and B. Li, *Materials science & engineering. C, Materials for biological applications*, 2014, **35**, 426-433.
37. J. Wei, S. J. Heo, D. H. Kim, S. E. Kim, Y. T. Hyun and J. W. Shin, *Journal of the Royal Society, Interface / the Royal Society*, 2008, **5**, 617-630.
38. Z. Lu, G. Wang, I. Roohani-Esfahani, C. R. Dunstan and H. Zreiqat, *Tissue engineering. Part A*, 2014, **20**, 992-1002.
39. M. Y. Shie, H. C. Chang and S. J. Ding, *Journal of biomedical materials research. Part A*, 2014, **102**, 769-780.
40. A. I. Rodrigues, M. E. Gomes, I. B. Leonor and R. L. Reis, *Acta biomaterialia*, 2012, **8**, 3765-3776.
41. R. Du, T. Wu, W. Liu, L. Li, L. Jiang, W. Peng, J. Chang and Y. Zhu, *Journal of endodontics*, 2013, **39**, 1023-1029.
42. H. Li and J. Chang, *Acta biomaterialia*, 2013, **9**, 6981-6991.
43. D. Lu, C. Luo, C. Zhang, Z. Li and M. Long, *Biomaterials*, 2014, **35**, 3945-3955.
44. Z. Li, Y. Gong, S. Sun, Y. Du, D. Lu, X. Liu and M. Long, *Biomaterials*, 2013, **34**, 7616-7625.
45. C. Guiducci and F. M. Spiga, *Nat Methods*, 2013, **10**, 617-618.
46. S. Sripanyakorn, R. Jugdaohsingh, W. Dissayabutr, S. H. C. Anderson, R. P. H. Thompson and J. J. Powell, *Brit J Nutr*, 2009, **102**, 825-834.
47. D. M. Reffitt, R. Jugdaohsingh, R. P. H. Thompson and J. J. Powell, *J Inorg Biochem*, 1999, **76**, 141-147.
48. E. Bisse, T. Epting, A. Beil, G. Lindinger, H. Lang and H. Wieland, *Anal Biochem*, 2005, **337**, 130-135.
49. H. Robberecht, R. Van Cauwenbergh, V. Van Vlaslaer and N. Hermans, *Sci Total Environ*, 2009, **407**, 4777-4782.
50. F. Y. Leung and P. Edmond, *Clin Biochem*, 1997, **30**, 399-403.
51. N. Zhang, J. A. Molenda, S. Mankoci, X. Zhou, W. L. Murphy and N. Sahai, *Biomater Sci-Uk*, 2013, **1**, 1101-1110.
52. L. N. Niu, D. Watson, K. Thames, C. M. Primus, B. E. Bergeron, K. Jiao, E. A. Bortoluzzi, C. W. Cutler, J. H. Chen, D. H. Pashley and F. R. Tay, *Sci Rep-Uk*, 2015, **5**.
53. A. N. Abell, N. V. Jordan, W. Huang, A. Prat, A. A. Midland, N. L. Johnson, D. A. Granger, P. A. Mieczkowski, C. M. Perou, S. M. Gomez, L. Li and G. L. Johnson, *Cell stem cell*, 2011, **8**, 525-537.
54. M. Herberg, T. Zerjatke, W. de Back, I. Glauche and I. Roeder, *Cytometry. Part A : the journal of the International Society for Analytical Cytology*, 2015, DOI: 10.1002/cyto.a.22598.
55. L. Meseguer-Olmo, S. Aznar-Cervantes, P. Mazon and P. N. De Aza, *Journal of materials science. Materials in medicine*, 2012, **23**, 3003-3014.
56. H. Li, K. Xue, N. Kong, K. Liu and J. Chang, *Biomaterials*, 2014, **35**, 3803-3818.
57. J. J. Guan, J. Y. Zhang, S. C. Guo, H. Y. Zhu, Z. Z. Zhu, H. Y. Li, Y. Wang, C. Q. Zhang and J. Chang, *Biomaterials*, 2015, **55**, 1-11.
58. X. Zhao, W. He, Z. Song, Z. Tong, S. Li and L. Ni, *Mol Biol Rep*, 2012, **39**, 215-220.
59. X. M. Zhang, C. T. Wu, J. Chang and J. Sun, *J Mater Chem B*, 2014, **2**, 885-891.
60. W. H. Lien and E. Fuchs, *Gene Dev*, 2014, **28**, 1517-1532.
61. P. P. Han, C. T. Wu and Y. Xiao, *Biomater Sci-Uk*, 2013, **1**, 379-392.

Table of contents entry
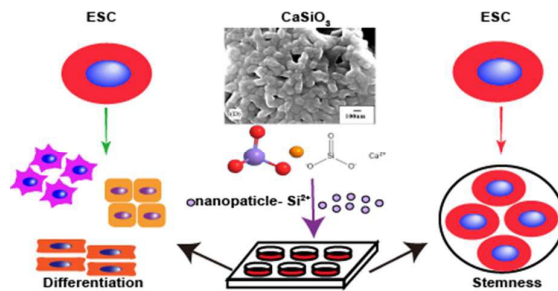
We shed a light on the impact of CS extracts on hESC's proliferation and differentiation, which is not clearly investigated.

RSC Advances Accepted Manuscript